Title: Assessing the real-time activation of the cannabinoid CB1 receptor and the associated structural changes using a FRET biosensor

Authors: Ying Liu, Lu-Yao Chen, Hong Zeng, Richard Ward, Nan Wu, Li Ma, Xi Mu, Qiu-Lan Li, Yang Yang, Su An, Xiao-Xi Guo, Qian Hao, Tian-Rui Xu

PII: S1357-2725(18)30078-5
DOI: https://doi.org/10.1016/j.biocel.2018.04.003
Reference: BC 5339

To appear in: *The International Journal of Biochemistry & Cell Biology*

Received date: 19-12-2017
Revised date: 25-3-2018
Accepted date: 4-4-2018

Please cite this article as: Liu Y, Chen L-Yao, Zeng H, Ward R, Wu N, Ma L, Mu X, Li Q-Lan, Yang Y, An S, Guo X-Xi, Hao Q, Xu T-Rui, Assessing the real-time activation of the cannabinoid CB1 receptor and the associated structural changes using a FRET biosensor, *International Journal of Biochemistry and Cell Biology* (2010), https://doi.org/10.1016/j.biocel.2018.04.003

Assessing the real-time activation of the cannabinoid CB1 receptor and the associated structural changes using a FRET biosensor

Ying Liu[a], Lu-Yao Chen[a], Hong Zeng[a], Richard Ward[b], Nan Wu[a], Li Ma[a], Xi Mu[a], Qiu-Lan Li[a], Yang Yang[a], Su An[a], Xiao-Xi Guo[a], Qian Hao[a], Tian-Rui Xu[a*]

[a]Faculty of Life Science and Technology, Kunming University of Science and Technology, Kunming, Yunnan, China 650500

[b]Center for Translational Pharmacology, Institute of Molecular, Cell and Systems Biology, College of Medical, Veterinary and Life Sciences, University of Glasgow, Glasgow G12 8QQ, Scotland, United Kingdom

Corresponding author: Tian-Rui Xu, the contact information are as follows:

Faculty of Life Science and Technology

Kunming University of Science and Technology, Kunming, Yunnan, China 650500

Email: tianruixu@kmust.edu.cn.

Abstract

The cannabinoid receptor 1 (CB1) is mainly expressed in the nervous system and regulates learning, memory processes, pain and energy metabolism. However, there is no way to directly measure its activation. In this study, we constructed a CB1 intramolecular fluorescence resonance energy transfer (FRET) sensor, which could measure CB1 activation by monitoring structural changes between the third intracellular loop and the C-terminal tail. CB1 agonists induced a time- and concentration-dependent increase in the FRET signal, corresponding to a reduction in the distance between the third intracellular loop and the C-terminal tail. This, in turn, mobilized intracellular Ca^{2+}, inhibited cAMP accumulation, and increased phosphorylation of the ERK1/2 MAP kinases. The activation kinetics detected using this method were consistent with those from previous reports. Moreover, the increased FRET signal was markedly inhibited by the CB1 antagonist rimonabant, which also reduced phosphorylation of the ERK1/2 MAP kinases. We mutated a single cysteine residue in the sensor (at position 257 or 264) to alanine. Both mutation reduced the agonist-induced increase in FRET signal and structural changes in the CB1 receptor, which attenuated phosphorylation of the ERK1/2 MAP kinases. In summary, our sensor directly assesses the kinetics of CB1 activation in real-time and can be used to monitor CB1 structure and function.

Key words: Cannabinoid receptor; ERK1/2 MAP kinase; FRET sensors; receptor activation; G protein-coupled receptor

1. Introduction

Endocannabinoids have important roles in various physiological and pathophysiological processes (Katona and Freund, 2012). They also act as ligands for G protein-coupled receptors

(GPCRs), including the cannabinoid type 1 receptor (CB1) and the CB2 receptor (Laprairie et al., 2016; Pertwee, 2008). These receptors are widely expressed in the brain (Liu et al., 2003), particularly in those regions that are involved in learning and memory processes (Morris, 2006). CB1 receptors are located at excitatory and inhibitory nerve terminals and CB1 activation directly inhibits neurotransmitter release, synapse formation, nociception, and appetite (Liu et al., 2003; Svizenska et al., 2008). Therefore, drugs targeting CB1 have been investigated as treatments for pain, energy metabolism, and movement disorders, including Huntington's disease (HD), Parkinson's disease, and other neurodegenerative and psychiatric conditions. Like all GPCRs, CB1 and CB2 possess seven transmembrane (TM) a-helical domains linked by three extracellular and three intracellular loops, an extracellular amino-terminal domain, and an intracellular carboxy-terminal domain. These domains create interacting regions for extracellular stimuli, including small molecules, hormones, peptides, lipids, and proteins. These interactions allow CB1 and CB2 to couple with heterotrimeric GTP binding-proteins (G proteins) (Moreira, 2014).

GPCRs are activated by ligand binding and undergo a conformational change that facilitates coupling with heterotrimeric G protein and subsequent activation. Activated G proteins then generate of second messengers such as cyclic adenosine monophosphate (cAMP), calcium, or phosphoinositides (Salazar et al., 2017; Surdo et al., 2017). The structure of GPCRs changes after activation (Bohme et al., 2008; Namkung et al., 2009) and, GPCR activation can be determined by observing these structural changes. Agonist-induced GPCR activation alters the conformation of the seven transmembrane α helices, particularly helices III and VI (Bissantz, 2003; Gether, 2000). Like many other GPCRs, the third intracellular (i3c) loop of is required for the coupling of CB1 with its major effector, the Gαi/o protein, which initiates receptor signaling and internalization (Turner et al., 2004). To investigate the impact of CB1 activation on receptor conformation and function, we prepared intramolecular fluorescence resonance energy transfer (FRET) sensors by inserting eYFP into the i3c loop and eCFP into the C-terminal domain of CB1.

Various methods for studying GPCR activation have been developed, such as the cAMP production assay (Storch et al., 2017), Ca^{2+} mobilization assay (Pennock and Hentges, 2016), ERK1/2 phosphorylation assay (Jain et al., 2016), and the β-arrestin recruitment assay (Alex

and Antunes, 2015; Soethoudt et al., 2016). However, these methods cannot detect GPCRs activation directly. FRET-based probes are useful for screening and have been used to investigate the kinetics of ligand binding and for other pharmacological analyses. Here, we constructed a CB1 FRET-based sensor to monitor ligand-induced CB1 activation during extracellular signal-regulated kinases 1 and 2 (ERK1/2) phosphorylation levels and receptor internalization. Small conformational changes induced by ligand binding are amplified at the cytoplasmic face of the CB1 receptor and, transmit signals to G proteins and other downstream effectors. This movement is detected by the FRET sensor.

In summary, we have constructed a system to monitor CB1 activation in real time by intramolecular FRET. FRET sensors may be used to screen a variety of important CB1 target drugs in the future.

2. Materials and methods

2.1. Materials

Doxycycline, WIN-55212-2, arachidonylethanolamide (ARA), CP-55940, rimonabant and monoclonal mouse anti-VSV-G antibodies were obtained from Sigma-Aldrich (Gillingham, UK). Lipofectamine 2000 transfection reagent was purchased from Invitrogen (Gibco, Germany). Protease inhibitor cocktail tablets were purchased from Millipore (Merck Millipore, Germany). Monoclonal rabbit p44/42 mitogen-activated protein kinase (MAPK; ERK1/2) and polyclonal rabbit phospho-p44/42 MAPK (phosphor-ERK1/2) antibodies were obtained from Cell Signaling Technology (UK). All other reagents were obtained from Thermo Fisher Scientific (Waltham, MA, USA) and Sigma Aldrich (Gillingham, UK).

2.2. DNA constructs

To generate intramolecular FRET sensors of the human CB1 receptor, eCFP (the energy donor), was inserted into the C-terminal region and eYFP (the energy acceptor), was inserted into the third intracellular loop (i3c). First, we generated a pcDNA5/FRT/TO-VSV-G- CB1-eCFP construct by replacing the Orexin-1 receptor sequence of pcDNA5/FRT/TO-VSV-G-h-Orexin-eCFP with the CB1 receptor sequence using the In-Fusion HD Cloning Kit (Clontech). A linearized vector was generated by PCR using the following primers: (sense) 5′-

ATGGTGAGCAAGGGCGAGG-3′; (antisense) 5′-CTTACCAA GGCGGTTCATTTCG-3′. Subsequently, CB1 receptor-specific primers with 15 bp extensions homologous to vector ends were designed: (sense) 5′-AACCGCCTTGGTAAGATGAAGTCGATCCTAGATGG-3′; (antisense) 5′- CACCATGGCGGCCGCCAGAGCCTCGGCAGACGTGT-3′. Subsequently, eYFP was inserted in the middle of the third CB1 receptor loop using the following primers: (sense) 5′- ATCATCATCCACACGATGGTGAGCAAGGGCGAGGA-3′; (antisense) 5′-CTTCCCATCCTCAGACTTGTACAGCTCGTCCATGC-3′.

2.3. Generation and maintenance of stable Flp-In™ T-REx™ 293 cells

To generate a Flp-In™ T-REx™ 293 cell line which inducible FRET sensor expression, parental Flp-In™ T-REx™ 293 cells were co-transfected with sensor constructs cloned into the pcDNA5/FRT/TO vector (as described above) and the pOG44 plasmid in a 1:9 ratio. Transfection was carried out using Lipofectamine 2000 (Invitrogen) according to the manufacturer's instructions. After 48 h, the medium was supplemented with 200 $\mu g.ml^{-1}$ hygromycin B to select for stably transfected cells. After approximately 10 days, colonies had appeared and were pooled. Cells were treated with 1 $\mu g.ml^{-1}$ doxycycline for 24 h to induce the expression of the desired protein. eCFP expression was detected by fluorescence imaging and VSV-G tagged protein expression was detected by western blotting.

2.4. Calcium assay

Intracellular Ca^{2+} release in cells stably expressing the CB1 sensor was measured using the Fluo-4 NW Calcium Assay Kit (Invitrogen) as previously described (Saini et al., 2010; Saini et al., 2011; Tripathi et al., 2013). Briefly, cells were grown on 18mm coverslips overnight until 80%-100% confluent. The coverslips were washed twice with modified Krebs solution (135 mM NaCl, 5.9 mM KCl, 1.5 mM $CaCl_2$, 1.2 mM $MgCl_2$, 11.5 mM glucose, 11.6 mM Hepes, pH 7.3) and then incubated in the same solution with 5 μM Fluo-4, 0.1% BSA for 30 min at 37°C in the dark followed by additional 30 min at room temperature in the dark. All other steps were performed at room temperature with continuous perfusion of bath solution (1× Hanks' balanced salt solution with 20 mM Hepes, pH 7.3) at a rate of 3.5 $ml.min^{-1}$. Cells were imaged using an Olympus inverted epifluorescence microscope (10× fluorescence objective) and

MetaMorph software (Vers.7.7.5 Molecular Devices, Sunnydale, CA). Fura-4 fluorescence (494 nm excitation, 516 nm emission) was measured every second for 1 min after the application of Hepes buffer or different agonists (concentration=10^{-6}M). For Ca^{2+} flux analyses, the agonist/buffer fluorescence ratio (F/F_0 ratio) was calculated for each cell and an averaged valued for all cells in the field of view was calculated.

2.5. Western blotting

Cells stably expressing the CB1 receptor sensor were serum-starved for 12 h and then stimulated with ligands at indicate concentrations and for lengths of time at 37°C. After stimulation, the cells were washed once in cold PBS and harvested in ice-cold RIPA buffer (Beyotime Biotechnology, China) supplemented with complete protease inhibitor mixture (Millipore Corporation). The cell lysates were centrifuged at 12000 × *g* for 15 min at 4°C and the protein content of the supernatant was determined using a BCA assay kit (Beyotime Biotechnology, China). Equivalent amounts of total proteins were separated by SDS-PAGE (on a 10% SDS gel) and transferred to polyvinylidene difluoride (PVDF) membranes. The membranes were blocked (5% fat-free milk powder in PBS with 0.1% Tween-20) at room temperature for 1 h and then incubated in primary antibodies diluted in block solution (5% fat-free milk powder in PBS) at a concentration of 1:1000-1:5000 at 4°C on a rocking shaker overnight. Subsequently, the membranes were washed three times in PBST buffer for a total of 30 min (3×10 min) and incubated for 1 h in appropriate secondary antibody diluted in block solution (1:10000) at room temperature. After washing, proteins were detected by enhanced chemiluminescence (Pierce Protein Research Products, Thermo Scientific) according to the manufacturer's instructions.

2.6. ERK1/2 MAP kinase phosphorylation

ERK1/2 MAP kinase phosphorylation was detected by protein immunoblotting using a phospho-ERK1/2-specific antibody (Cell Signaling Technology, Nottingham, UK). The PVDF membranes were stripped of immunoglobulins and re-probed using an anti-ERK1/2 antibody (Cell Signaling Technology, Nottingham, UK) to demonstrate equal protein loading.

2.7. Detection of internalization by fluorescence microscopy

To visualize WIN-55212-2-induced receptor internalization, cells stably expressing the CB1 receptor sensor were grown on cover slips and incubated in a microscope chamber containing physiological HEPES-buffered saline solution (130 mM NaCl, 5 mM KCl, 1 mM $CaCl_2$, 1 mM $MgCl_2$, 20 mM HEPES, and 10 mM D-glucose, pH 7.4) and treated with 1×10^{-6} M WIN-55212-2 for indicate time periods. The effect of eCFP insertion on receptor distribution between the cell surface and cytoplasm was assessed using an inverted Olympus microscope.

2.8. Biotinylation internalization assay

Stably transfected CB1 sensor cells were grown in 6-well plates pre-coated with 0.1 $ng.ml^{-1}$ poly-D-lysine and induced overnight with 100 $ng.ml^{-1}$ doxycycline. Cells were then treated with specific ligands. After treatment, the plates were put on ice, the medium was removed, and the cells were washed with ice-cold borate buffer (10 mM boric acid, 154 mM NaCl, 7.2 mM KCl, 1.8 mM $CaCl_2$, pH 9.0; 2 ml/well). Subsequently, 1 ml/well of 0.8 mM Sulfo-NHS-SS-Biotin (Pierce, Thermo Scientific) in borate buffer was added and the plates were incubated on ice in the dark for a further 30 min. After removing the biotin solution, the cells were washed with stop solution (192 mM glycine, 25 mM Tris-HCl, pH 8.3) and then incubated with 2 ml/well stop solution for 5 min on ice. Subsequently, the stop solution was removed and the cells were lysed in 500–1000 µl RIPA lysis buffer and placed on ice for 15 min. The cell lysates were transferred to microcentrifuge tubes and centrifuged at 18,000 × *g* for 10 min at 4 °C. Streptavidin-agarose resin (100 µl/tube) (Pierce, Thermo Scientific) was then added and tubes were incubated on a rotating wheel at 4 °C overnight followed by centrifugation at 2000 × *g* for 2 min at 4 °C. The supernatant was removed and the resin was washed with three times in 500 µl RIPA buffer. Next, 100 µl SDS-PAGE sample buffercontaining 5% β-mercaptoethanol was added and tubes were incubated at 37 °C for 1 h. The cell lysates and biotinylated samples were analyzed by SDS-PAGE and western blotting as described above.

2.9. FRET imaging

FRET was visualized in cells growing in 6-wells plates using an inverted Olympus microscope (Olympus Instruments) equipped with a 40× (numerical aperture = 1.3) oil immersion Fluor lens. For FRET experiments, the monochromator was set to 427 nm

bandwidth to visualize surface CFP-tagged receptors labeled with YFP. Excitation light (427 nm or 504 nm) was reflected through the Fluor objective lens using a cyan/yellow fluorescent protein dual band dichroic filter mounted in the microscope. FRET and donor emission images were recorded at exactly the same time interval using a QV2 image splitting device coupled to a Cool Snap-HQ2 camera, which was connected to the bottom port for maximal fluorescence detection. FRET was detected simultaneously using the following QV2 cubes: ET 535/30 nm, ET 470/30 nm, and ET 632/60 nm. Using the streaming capability of the multidimensional wavelength acquisition MetaMorph module, ligand-induced changes in intramolecular FRET were recorded directly to a computer hard drive at 40 ms intervals during excitation with 427 nm light. The Cool Snap-HQ2 camera was operated in 14-bit mode. The exposure times, binning (8 × 8) and camera gain were kept constant for all streaming experiments.

2.10. Calculation of FRET efficiency

All images were analyzed using MetaMorph (Molecular Devices). An eCFP-eYFP reference construct with known FRET efficiency was used for calibration in each experiment. Ratiometric FRET values were then calculated as the average 535 nm emission intensity divided by the average 470 nm emission intensity. The quantified FRET ratios were exported to Prism 5.02 (GraphPad Software Inc., San Diego, CA) and set to 1.0 using the transforming module of the software and plotted over time. Control experiments were performed to ensure that the X-Rhod-1 dye-emitted fluorescence did not bleed into the donor or FRET channel of the QV2 image splitter. No emitted eCFP or eYFP fluorescence was detected in the 630 nm emission channel of the QV2. The 470/535 FRET ratio is directly proportional to the cellular redox potential (Xu et al., 2012).

2.11. Data analysis

All data were analyzed using Prism 5.01 (GraphPad Software Inc., San Diego, CA). *K*on represents the observed ligand association rate constant. *K*off represents the observed ligand dissociation rate constant. *K*d denotes the affinity constant of the ligand and was calculated as the ratio of *K*on and *K*off. Values are given as means ± S.E.M. of n independent experiments. Statistical comparisons between parameters were performed using Student's t test. A p value of

<0.05 was taken as significant.

3. Results

3.1 Generation of receptor sensor constructs

We used a CB1 sensor to detect and monitor CB1 activation in living cells. The sensor was constructed by fusing eCFP to the C-terminal tail of full-length human CB1 with a VSV-G tag sequence in the extracellular N-terminal domain (Fig. 1A). eYFP was inserted into the full-length i3c loop (22 and 23 amino acids of the CB1 receptor i3c loop flanking the eYFP (Fig. 1B)). To demonstrate that eCFP and eYFP fluoresce in our receptor construct, we transiently transfected the construct into HEK 293T cells. The cells were excited at 430 nm for eCFP and 520 nm for eYFP and then monitored using a confocal microscope. We observed localized fluorescence at the cell membrane following excitation of eCFP and eYFP (Fig. 1C).

3.2 Agonist-dependent changes in FRET signals

We evaluated the FRET signal of the intramolecular sensor by measuring changes in FRET efficiency in stable cells. Upon activation by the agonist WIN-55212-2, time- and concentration-dependent increases in FRET efficiency were observed (Fig. 1D).

To further explore the relationship between change in conformation and activity, we investigated the effect of rimonabant, an antagonist of the CB1 receptor, on CB1 activation. Pre-incubation with 10^{-6} M rimonabant, largely blocked the effect of WIN-55212-2 (10^{-6} M)-induced CB1 activation (Fig. 1E). Notably, rimonabant-induced changes in FRET signal were similar to the correlation between activity and FRET conformation.

Important parameters of GPCR activation are the agonist binding kinetics. These include the association rate constant (*K*on), the dissociation rate constant (*K*off), and the equilibrium binding constant (*K*d). As well as the kinetics of receptor activation, we were also interested in the dissociation constants of the receptor. The kinetics of receptor activation were analyzed by recording FRET signals after activation with various concentrations of WIN-55212-2 (Table. 1).

Further FRET imaging experiments showed marked changes in FRET signal upon application of ARA (Fig. 2A) and CP-55940 (Fig. 2B). ARA is an endogenous agonist of the

CB1 receptor and caused an equilibrium binding constant (*Kd*) of 7.108 ± 0.062 nM, similar to WIN-55212-2 (*Kd*=7.067 ± 0.012 nM) (Table. 2). Furthermore, pretreatment with the allosteric modulator Org27569 (Fig. 2C) or inverse agonist taranabant (Fig. 2D) reduced WIN-55212-2-induced changes in FRET signal.

3.3. A CB1 agonist induces intracellular Ca^{2+} mobilization

We investigated whether changes in the FRET signal correlated with downstream intracellular signals and examined whether the kinetics of receptor activation were similar to those of induced intracellular Ca^{2+} flux. Within 60 seconds of CB1 receptor activation 10^{-6} M WIN-55212-2 (Fig. 3A), arachidonylethanolamide (Fig. 3B), and CP-55940 (Fig. 3C) elevated intracellular Ca^{2+} concentrations by more than 1.5-fold. However, elevation of intracellular Ca^{2+} mobilization was reduced by pretreatment with Org27569 (Fig. 3D) or taranabant (Fig. 3E).

In comparison, alteration in sensor FRET signals were detected within 1 s of agonist addition (10^{-6} M) (Fig. 1D). However, it took 8-10 s longer to detect changes in Ca^{2+} concentration ($p<0.001$) (Fig. 3). It is currently not clear why a similar structural change (as reported by the FRET sensor) induces different Ca^{2+} activation patterns; this should be studied further study. Our results clearly show that the signal response from the FRET sensor is at least as sensitive to the ligand as the Ca^{2+} response following treatment with different agonists at the same concentration.

3.4. CB1 biosensor internalization after activation

During chronic agonist stimulation, the signal generated by activated GPCRs often diminishes through desensitization, which uncouples the receptor from its downstream signaling cascade (Blume et al., 2016). GPCR internalization has long been considered a major aspect of the desensitization process (Snyder et al., 2013). Internalization contributes to the diversity of GPCR-dependent signaling, including G protein-dependent cAMP accumulation (Kotowski et al., 2011), cAMP-response element-binding protein (CREB) phosphorylation (Tsvetanova and von Zastrow, 2014), adenylyl cyclase inhibition (Ferguson, 2001), and protein kinase C (PKC) activation (Bailey et al., 2009; Zheng et al., 2008). The dynamics and quantification of GPCR internalization in living cells has generated considerable interest.

Firstly, to demonstrate agonist-induced movement of the receptor from the cell surface to intracellular vesicles, we monitored eCFP (Fig. 4A) using fluorescence microscopy. The eCFP signal gradually moved from the cell surface to the intracellular region in a time-dependent manner, indicating receptor internalization.

In order to quantify receptor internalization and measure the potency of WIN-55212-2, we performed cell surface biotinylation studies. CB1 receptor sensor-expressing cells (Fig. 4B-C) were either treated with 10^{-6} M WIN-55212-2 for up to 60 min or with varying doses of WIN-55212-2 for 40 min, next, biotin-labeled cell surface proteins were captured by immobilized streptavidin, separated by SDS-PAGE, and analyzed by western blotting using an anti-VSV-G antibody to detect the FRET sensor. In Figures 4B-C, we identified an apparently single polypeptide of 80 kDa in the absence of WIN-55212-2. Increasing exposure and dose of WIN-55212-2 treatment reduced the level of biotinylated polypeptide detected by the anti-VSV-G antibody, consistent with the removal of receptor from the cell surface. These findings confirmed that the FRET signal records the agonist-induced activation of the receptor rather than a downstream-mediated effect.

3.5. CB1 sensor activation results in phosphorylation of ERK1/2 MAP kinase

To determine whether CB1 activation causes phosphorylation of ERK1/2 MAP kinase, we examined ERK1/2 MAP kinase phosphorylation by western blot analysis. Cells expressing the CB1 receptor sensor were incubated with varying concentrations of WIN-55212-2 or ARA for 5 min and then cell lysates were separated by SDS-PAGE. PVDF membranes were immunoblotted with anti-VSV-G and anti-p-ERK1/2 antibodies. As shown in Fig. 5A and C, VSV-G sensor expression was significantly induced by doxycycline administration in a WIN-55212-2-independent and ARA-independent manner. Furthermore, WIN-55212-2 or ARA treatment significantly increased the phosphorylation of ERK1/2 MAP kinase in a dose-dependent manner (Figure 5B, D). These results demonstrated that activation of the CB1 sensor activates the ERK1/2 MAP kinase signaling pathway.

3.6. CB1 sensor activation-induced ERK1/2 MAP kinase phosphorylation is partially blocked by a CB1 agonist and by mutations that prevent agonist binding

To further examine the phosphorylation of ERK1/2 MAP kinase induced by FRET sensor activation, cells were pre-treated with rimonabant for 20 minutes then stimulated with different agonists. ERK1/2 MAP kinase phosphorylation was analyzed by western blotting. As shown in Fig. 6, pretreatment with rimonabant for 20 min markedly inhibited ERK1/2 MAP kinase phosphorylation induced by WIN-55212-2 (Fig. 6A), ARA (Fig. 6B) and CPA (Fig. 6C). These results indicate that activation of the CB1 FRET-based sensor can be blocked by a CB1 antagonist/inverse agonist and that this, in turn, reduces ERK1/2 MAP kinase phosphorylation.

Previous studies have shown that mutation of residues Cys-257 to Ala or Cys-264 to Ala in the CB1 receptor impairs its ability to bind to ligands (Fay and Farrens, 2013). We introduced these two mutations (separately) into the mGluR5-VSV-G-CB1-YFP-CFP sensor and into doxycycline-inducible stable cells lines. Analysis of these cell lines showed that high concentrations of WIN-55212-2 (1×10^{-6} M) only had small effects on ERK1/2 MAP kinase phosphorylation compared with unmutated FRET sensors (Fig. 6D). This suggests, consistent with the loss of agonist binding, that these mutations block the response of FRET sensor to WIN-55212-2.

4. Discussion

The most basic function of a GPCR is activation by agonist binding, which couples to the receptor to results in coupling to (in many cases) a G protein, thus propagating a variety of cell signaling cascades (Kobilka and Deupi, 2007; Rasmussen et al., 2011; Rovati et al., 2007). GPCRs contain multiple regions that couple the receptor to signal transduction complexes. The most prominent of these domains are the second (i2c) and third (i3c) intracellular loops as well as the C-terminal tail and TM boundaries (Ratnala and Kobilka, 2009; Rosenbaum et al., 2009; Williams and Hill, 2009). Recently, X-ray analysis revealed the structure of GPCRs in their active and inactive states. These analyses showed that GPCRs undergo conformational changes after activation, causing certain domains to move. Movement was most prominent helix VI, followed by helix V, and then the C-terminal (Kruse et al., 2013). These movements can be monitored by intramolecular FRET sensors in a number of GPCRs (Alvarez-Curto et al., 2011; Chachisvilis et al., 2006; Hoffmann et al., 2005; Ilien et al., 2003; Maier-Peuschel et al., 2010;

Vilardaga et al., 2003). In this approach, ligand binding and subsequent receptor activation alters the relative orientation of the fluorophores inserted into the C-terminus and third intracellular loop of the receptor, therefore FRET signal (Malik et al., 2013). Based on the anticipated movements of transmembrane helices V and VI in response to agonist binding, these receptor constructs have all introduced a FRET reporter into the i3c loop, which links these helices. The FRET partners were placed at or within the C-terminal tail (Fig. 1A). Using YFP in combination with CFP in a FRET-based GPCR probe is a well-established method to monitor conformational changes upon receptor activation and ligand–receptor binding (Fig. 2) and illustrates the potential uses of small fluorescent marker in labeling defined proteins in living cells (Adjobo-Hermans et al., 2011; Sinha et al., 2014).

Unimolecular GPCR-based FRET sensors can detect ligand binding (Ma et al., 2014; Manglik et al., 2015; Vilardaga et al., 2013; Ward and Milligan, 2014). Yu Bin et al. used a FRET-based biosensor to detect cAMP levels in *C. elegans* and measure spatiotemporal changes in ATP. To directly examine changes in cAMP levels in GABAergic motor neurons of *C. elegans*, they used an exchange protein directly activated by cAMP (EPAC) to express a FRET construct correlated inversely with the cellular cAMP levels (Yu et al., 2017). In another study, Kim HJ et al. developed a ratiometric two-photon fluorescent probe (SCa1-I_{REF}) containing two fluorophores with different Stokes shifts to image Ca^{2+} in live neurons and various tissues. These probes are better for Ca2+ imaging than traditional intramolecular charge transfer-based and FRET-based probes, which are based on a turn-on sensing process and are limited to quantitative detection (Kim et al., 2017). Zoghbi ME et al. used luminescence resonance energy transfer (LRET) to measure the distances between the two P-glycoprotein (Pgp) nucleotide-binding domains. LRET, like the traditional FRET, is based on energy transfer from a donor to an acceptor. However, LRET uses a lanthanide (Tb^{3+} or Eu^{3+}) as a donor. Luminescent lanthanides are better suited than FRET donors for membrane protein studies (Zoghbi et al., 2017). The principle behind the above-mentioned biosensors is the same as that of the FRET sensor presented here.

GPCR-based FRET sensors provide information on the kinetics of GPCR responses to different ligands. Such constructs have recently been used to detect alterations in receptor responses to orthosteric and allosteric ligands (Hoffmann et al., 2010). The dynamic transitions

between different receptor states appear to be important for receptor function (Manglik et al., 2015). In this study, we present an effective method to detect CB1 activation directly, by observing its structural changes. Notably, these structural changes were consistent with the activation of downstream signaling effectors.

The on-rate of ligand binding to a receptor depends upon the ligand concentration and the on-rate constant (Kon, expressed in M^{-1} s^{-1}). The off-rate of ligand binding is independent of ligand concentration and the off-rate constant (Koff, expressed in s^{-1}). In the present study, agonist binding to CB1 sensors activation in a concentration-dependent manner (Fig. 1-2). This is consistent with previous findings that adenosine binding to an adenosine A2A receptor-based FRET sensor increased receptor activation in a concentration-dependent manner (Hoffmann et al., 2005).

The present study has shown that different agonists induce different conformational changes in living cells (Fig. 1-2). The agonist WIN-55212,2, arachidonylethanolamide and CP-55940 induced marked conformational changes in living cells. The allosteric modulator org27569 or the inverse agonist taranabant inhibited WIN-55212,2-induced conformational changes (Fig. 1-2). Moreover, our FRET-based CB1 receptor biosensor successfully monitored Ca^{2+} in real-time in live cells (Fig. 3). Agonist-induced GPCR internalization is a largely ubiquitous process (Irannejad et al., 2013; Pampillo and Babwah, 2015) and its regulation is complex (Levoye et al., 2015), which suggests that it is biologically important. Receptor internalization was generally thought to play a role in adaptation and down-regulation. However, it may be a prelude to continued intracellular receptor activity (Ayoub and Pfleger, 2010). In the present study, we have shown that WIN-55212-2-induced activation of our CB1 FRET-based sensor is followed by internalization (Fig. 4). GPCR-based FRET sensors have many uses, including allosteric modulators (Bolognini et al., 2016; Hill et al., 2014), investigation of receptor dimers (Adjobo-Hermans et al., 2011), and studying constitutive receptor activity (Hoffmann et al., 2005). Much has been learned about GPCR pharmacology and biology through the use of such sensors, therefore the effort involved in making them is worthwhile.

The CB1 FRET sensor can be to estimate the effect of different compounds on the receptor directly, for example in drug screening. FRET-based GPCR sensors can increase the distance between YFP and CFP by 10^6 ($E=R_0^6/R_0^6+R^6$). Inactive compounds do not alter the

spatiotemporal conformation of the receptors they bind to, therefore do not change the FRET signal (Lohse et al., 2012). However, active compounds (or agonists) alter the spatiotemporal conformation of the receptors they bind to and thereby change the FRET signal. This approach may provide a simple readout for drug screening that is not affected by the cell state or other signaling pathways.

Although it is an incredibly useful tool, FRET is not without shortcomings. Firstly, the probes are small have limited use in live sample imaging because of turn-on sensing and single detection window, fast photobleaching, short excitation light, potential for photodamage, and limited tissue penetration (Lombardi et al., 2017; Zadran et al., 2012). Secondly, the reaction is irreversible, so is limited to visualizing the dynamic concentration change of the analyte (Leavesley et al., 2015). Thirdly, the number of fluorescent tag proteins that can be used in combination is limited. The donor emission range and the acceptor excitation range have to overlap by at least 30%, otherwise, auto-fluorescence may interfere with the FRET data (Lovell et al., 2009).

Overall, the present study provides a direct method for detecting CB1 activation by monitoring structural changes. Our CB1-based FRET sensor can also be used to analyze various cellular processes, such as activation kinetics, allosteric modulation, and receptor dimerization.

Conflict of interest statement

The authors declare no conflicts of interest.

Acknowledgments

This work was funded by the NSFC (81473342, 81560455, U1302225, 81460417, 81460253).

Abbreviations

CB1, cannabinoid type 1 receptor; FRET, fluorescence resonance energy transfer; GPCRs, G protein-coupled receptors; HD, Huntington's disease; TM, transmembrane; G-proteins, GTP binding-proteins; cAMP, cyclic adenosine monophosphate; ERK1/2, extracellular signal-regulated kinases 1 and 2; PVDF, polyvinylidene difluoride; *K*on, the association rate constant; *K*off, the dissociation rate constant; *K*d, the equilibrium binding constant; CREB; cAMP-response element-binding protein; i3 loop, the third intracellular loop.

References

Adjobo-Hermans, M.J., Goedhart, J., van Weeren, L., Nijmeijer, S., Manders, E.M., Offermanns, S., Gadella, T.W., Jr., 2011. Real-time visualization of heterotrimeric G protein Gq activation in living cells. BMC biology 9, 32.

Alex, A., Antunes, A., 2015. Pyrosequencing characterization of the microbiota from Atlantic intertidal marine sponges reveals high microbial diversity and the lack of co-occurrence patterns. PloS one 10(5), e0127455.

Alvarez-Curto, E., Prihandoko, R., Tautermann, C.S., Zwier, J.M., Pediani, J.D., Lohse, M.J., Hoffmann, C., Tobin, A.B., Milligan, G., 2011. Developing chemical genetic approaches to explore G protein-coupled receptor function: validation of the use of a receptor activated solely by synthetic ligand (RASSL). Molecular pharmacology 80(6), 1033-1046.

Ayoub, M.A., Pfleger, K.D., 2010. Recent advances in bioluminescence resonance energy transfer technologies to study GPCR heteromerization. Current opinion in pharmacology 10(1), 44-52.

Bailey, C.P., Llorente, J., Gabra, B.H., Smith, F.L., Dewey, W.L., Kelly, E., Henderson, G., 2009. Role of protein kinase C and mu-opioid receptor (MOPr) desensitization in tolerance to morphine in rat locus coeruleus neurons. The European journal of neuroscience 29(2), 307-318.

Bissantz, C., 2003. Conformational changes of G protein-coupled receptors during their activation by agonist binding. Journal of receptor and signal transduction research 23(2-3), 123-153.

Blume, L.C., Leone-Kabler, S., Luessen, D.J., Marrs, G.S., Lyons, E., Bass, C.E., Chen, R., Selley, D.E., Howlett, A.C., 2016. Cannabinoid receptor interacting protein suppresses agonist-driven CB1 receptor internalization and regulates receptor replenishment in an agonist-biased manner. Journal of neurochemistry 139(3), 396-407.

Bohme, I., Stichel, J., Walther, C., Morl, K., Beck-Sickinger, A.G., 2008. Agonist induced receptor internalization of neuropeptide Y receptor subtypes depends on third intracellular loop and C-terminus. Cellular signalling 20(10), 1740-1749.

Bolognini, D., Moss, C.E., Nilsson, K., Petersson, A.U., Donnelly, I., Sergeev, E., Konig, G.M., Kostenis, E., Kurowska-Stolarska, M., Miller, A., Dekker, N., Tobin, A.B., Milligan, G., 2016. A Novel Allosteric Activator of Free Fatty Acid 2 Receptor Displays Unique Gi-functional Bias. The Journal of biological chemistry 291(36), 18915-18931.

Chachisvilis, M., Zhang, Y.L., Frangos, J.A., 2006. G protein-coupled receptors sense fluid shear stress in endothelial cells. Proceedings of the National Academy of Sciences of the United States of America 103(42), 15463-15468.

Fay, J.F., Farrens, D.L., 2013. The membrane proximal region of the cannabinoid receptor CB1 N-terminus can allosterically modulate ligand affinity. Biochemistry 52(46), 8286-8294.

Ferguson, S.S., 2001. Evolving concepts in G protein-coupled receptor endocytosis: the role in receptor desensitization and signaling. Pharmacological reviews 53(1), 1-24.

Gether, U., 2000. Uncovering molecular mechanisms involved in activation of G protein-coupled receptors. Endocrine reviews 21(1), 90-113.

Hill, S.J., May, L.T., Kellam, B., Woolard, J., 2014. Allosteric interactions at adenosine A(1) and A(3) receptors: new insights into the role of small molecules and receptor dimerization. British journal of pharmacology 171(5), 1102-1113.

Hoffmann, C., Gaietta, G., Bunemann, M., Adams, S.R., Oberdorff-Maass, S., Behr, B., Vilardaga, J.P., Tsien, R.Y., Ellisman, M.H., Lohse, M.J., 2005. A FlAsH-based FRET approach to determine G protein-coupled receptor activation in living cells. Nature methods 2(3), 171-176.

Hoffmann, C., Gaietta, G., Zurn, A., Adams, S.R., Terrillon, S., Ellisman, M.H., Tsien, R.Y., Lohse, M.J., 2010. Fluorescent labeling of tetracysteine-tagged proteins in intact cells. Nature protocols 5(10), 1666-1677.

Ilien, B., Franchet, C., Bernard, P., Morisset, S., Weill, C.O., Bourguignon, J.J., Hibert, M., Galzi, J.L., 2003. Fluorescence resonance energy transfer to probe human M1 muscarinic receptor structure and drug binding properties. Journal of neurochemistry 85(3), 768-778.

Irannejad, R., Tomshine, J.C., Tomshine, J.R., Chevalier, M., Mahoney, J.P., Steyaert, J., Rasmussen, S.G., Sunahara, R.K., El-Samad, H., Huang, B., von Zastrow, M., 2013. Conformational biosensors reveal GPCR signalling from endosomes. Nature 495(7442), 534-538.

Jain, R., Watson, U., Saini, D.K., 2016. ERK activated by Histamine H1 receptor is anti-proliferative through spatial restriction in the cytosol. European journal of cell biology 95(12), 623-634.

Katona, I., Freund, T.F., 2012. Multiple functions of endocannabinoid signaling in the brain. Annual review of neuroscience 35, 529-558.

Kim, H.J., Lim, C.S., Lee, H.W., Lee, H.S., Um, Y.J., Kumar, H., Han, I., Kim, H.M., 2017. A ratiometric two-photon probe for Ca(2+) in live tissues and its application to spinal cord injury model. Biomaterials 141, 251-259.

Kobilka, B.K., Deupi, X., 2007. Conformational complexity of G-protein-coupled receptors. Trends in pharmacological sciences 28(8), 397-406.

Kotowski, S.J., Hopf, F.W., Seif, T., Bonci, A., von Zastrow, M., 2011. Endocytosis promotes rapid dopaminergic signaling. Neuron 71(2), 278-290.

Kruse, A.C., Ring, A.M., Manglik, A., Hu, J., Hu, K., Eitel, K., Hubner, H., Pardon, E., Valant, C., Sexton, P.M., Christopoulos, A., Felder, C.C., Gmeiner, P., Steyaert, J., Weis, W.I., Garcia, K.C., Wess, J., Kobilka, B.K., 2013. Activation and allosteric modulation of a muscarinic acetylcholine receptor. Nature 504(7478), 101-106.

Laprairie, R.B., Bagher, A.M., Kelly, M.E., Denovan-Wright, E.M., 2016. Biased Type 1 Cannabinoid Receptor Signaling Influences Neuronal Viability in a Cell Culture Model of Huntington Disease. Molecular pharmacology 89(3), 364-375.

Leavesley, S.J., Nakhmani, A., Gao, Y., Rich, T.C., 2015. Automated image analysis of FRET signals for subcellular cAMP quantification. Methods in molecular biology 1294, 59-70.

Levoye, A., Zwier, J.M., Jaracz-Ros, A., Klipfel, L., Cottet, M., Maurel, D., Bdioui, S., Balabanian, K., Prezeau, L., Trinquet, E., Durroux, T., Bachelerie, F., 2015. A Broad G Protein-Coupled Receptor Internalization Assay that Combines SNAP-Tag Labeling, Diffusion-Enhanced Resonance Energy Transfer, and a Highly Emissive Terbium Cryptate. Frontiers in endocrinology 6, 167.

Liu, P., Bilkey, D.K., Darlington, C.L., Smith, P.F., 2003. Cannabinoid CB1 receptor protein expression in the rat hippocampus and entorhinal, perirhinal, postrhinal and temporal cortices: regional variations and age-related changes. Brain research 979(1-2), 235-239.

Lohse, M.J., Nuber, S., Hoffmann, C., 2012. Fluorescence/bioluminescence resonance energy transfer techniques to study G-protein-coupled receptor activation and signaling. Pharmacological reviews 64(2), 299-336.

Lombardi, A., Trimarco, B., Iaccarino, G., Santulli, G., 2017. Impaired mitochondrial calcium uptake caused by tacrolimus underlies beta-cell failure. Cell communication and signaling : CCS 15(1), 47.

Lovell, J.F., Chen, J., Jarvi, M.T., Cao, W.G., Allen, A.D., Liu, Y., Tidwell, T.T., Wilson, B.C., Zheng, G., 2009. FRET quenching of photosensitizer singlet oxygen generation. The journal of physical chemistry. B 113(10), 3203-3211.

Ma, Z., Du, L., Li, M., 2014. Toward fluorescent probes for G-protein-coupled receptors (GPCRs). Journal of medicinal chemistry 57(20), 8187-8203.

Maier-Peuschel, M., Frolich, N., Dees, C., Hommers, L.G., Hoffmann, C., Nikolaev, V.O., Lohse, M.J., 2010. A fluorescence resonance energy transfer-based M2 muscarinic receptor sensor reveals rapid kinetics of allosteric modulation. The Journal of biological chemistry 285(12), 8793-8800.

Malik, R.U., Ritt, M., DeVree, B.T., Neubig, R.R., Sunahara, R.K., Sivaramakrishnan, S., 2013. Detection of G protein-selective G protein-coupled receptor (GPCR) conformations in live cells. The Journal of biological chemistry 288(24), 17167-17178.

Manglik, A., Kim, T.H., Masureel, M., Altenbach, C., Yang, Z., Hilger, D., Lerch, M.T., Kobilka, T.S., Thian, F.S., Hubbell, W.L., Prosser, R.S., Kobilka, B.K., 2015. Structural Insights into the Dynamic Process of beta2-Adrenergic Receptor Signaling. Cell 161(5), 1101-1111.

Moreira, I.S., 2014. Structural features of the G-protein/GPCR interactions. Biochimica et biophysica acta 1840(1), 16-33.

Morris, R.G., 2006. Elements of a neurobiological theory of hippocampal function: the role of synaptic plasticity, synaptic tagging and schemas. The European journal of neuroscience 23(11), 2829-2846.

Namkung, Y., Dipace, C., Javitch, J.A., Sibley, D.R., 2009. G protein-coupled receptor kinase-mediated phosphorylation regulates post-endocytic trafficking of the D2 dopamine receptor. The Journal of biological chemistry 284(22), 15038-15051.

Pampillo, M., Babwah, A.V., 2015. Quantifying GPCR internalization: a focus on the Kisspeptin receptor. Methods in molecular biology 1272, 119-132.

Pennock, R.L., Hentges, S.T., 2016. Desensitization-resistant and -sensitive GPCR-mediated inhibition of GABA release occurs by Ca2+-dependent and -independent mechanisms at a hypothalamic synapse. Journal of neurophysiology 115(5), 2376-2388.

Pertwee, R.G., 2008. Ligands that target cannabinoid receptors in the brain: from THC to anandamide and beyond. Addiction biology 13(2), 147-159.

Rasmussen, S.G., DeVree, B.T., Zou, Y., Kruse, A.C., Chung, K.Y., Kobilka, T.S., Thian, F.S., Chae, P.S., Pardon, E., Calinski, D., Mathiesen, J.M., Shah, S.T., Lyons, J.A., Caffrey, M., Gellman, S.H., Steyaert, J., Skiniotis, G., Weis, W.I., Sunahara, R.K., Kobilka, B.K., 2011. Crystal structure of the beta2 adrenergic receptor-Gs protein complex. Nature 477(7366), 549-555.

Ratnala, V.R., Kobilka, B., 2009. Understanding the ligand-receptor-G protein ternary complex for GPCR drug discovery. Methods in molecular biology 552, 67-77.

Rosenbaum, D.M., Rasmussen, S.G., Kobilka, B.K., 2009. The structure and function of G-protein-coupled receptors. Nature 459(7245), 356-363.

Rovati, G.E., Capra, V., Neubig, R.R., 2007. The highly conserved DRY motif of class A G protein-coupled receptors: beyond the ground state. Molecular pharmacology 71(4), 959-964.

Saini, V., Marchese, A., Majetschak, M., 2010. CXC chemokine receptor 4 is a cell surface receptor for extracellular ubiquitin. The Journal of biological chemistry 285(20), 15566-15576.

Saini, V., Staren, D.M., Ziarek, J.J., Nashaat, Z.N., Campbell, E.M., Volkman, B.F., Marchese, A., Majetschak, M., 2011. The CXC chemokine receptor 4 ligands ubiquitin and stromal cell-derived factor-1alpha function through distinct receptor interactions. The Journal of biological chemistry

286(38), 33466-33477.

Salazar, A.I., Carozzo, A., Correa, F., Davio, C., Franchi, A.M., 2017. Evidence for CB2 receptor involvement in LPS-induced reduction of cAMP intracellular levels in uterine explants from pregnant mice: pathophysiological implications. Molecular human reproduction 23(7), 500-508.

Sinha, C., Arora, K., Moon, C.S., Yarlagadda, S., Woodrooffe, K., Naren, A.P., 2014. Forster resonance energy transfer - an approach to visualize the spatiotemporal regulation of macromolecular complex formation and compartmentalized cell signaling. Biochimica et biophysica acta 1840(10), 3067-3072.

Snyder, J.C., Rochelle, L.K., Lyerly, H.K., Caron, M.G., Barak, L.S., 2013. Constitutive internalization of the leucine-rich G protein-coupled receptor-5 (LGR5) to the trans-Golgi network. The Journal of biological chemistry 288(15), 10286-10297.

Soethoudt, M., van Gils, N., van der Stelt, M., Heitman, L.H., 2016. Protocol to Study beta-Arrestin Recruitment by CB1 and CB2 Cannabinoid Receptors. Methods in molecular biology 1412, 103-111.

Storch, U., Straub, J., Erdogmus, S., Gudermann, T., Mederos, Y.S.M., 2017. Dynamic monitoring of Gi/o-protein-mediated decreases of intracellular cAMP by FRET-based Epac sensors. Pflugers Archiv : European journal of physiology 469(5-6), 725-737.

Surdo, N.C., Berrera, M., Koschinski, A., Brescia, M., Machado, M.R., Carr, C., Wright, P., Gorelik, J., Morotti, S., Grandi, E., Bers, D.M., Pantano, S., Zaccolo, M., 2017. FRET biosensor uncovers cAMP nano-domains at beta-adrenergic targets that dictate precise tuning of cardiac contractility. Nature communications 8, 15031.

Svizenska, I., Dubovy, P., Sulcova, A., 2008. Cannabinoid receptors 1 and 2 (CB1 and CB2), their distribution, ligands and functional involvement in nervous system structures--a short review. Pharmacology, biochemistry, and behavior 90(4), 501-511.

Tripathi, A., Saini, V., Marchese, A., Volkman, B.F., Tang, W.J., Majetschak, M., 2013. Modulation of the CXC chemokine receptor 4 agonist activity of ubiquitin through C-terminal protein modification. Biochemistry 52(24), 4184-4192.

Tsvetanova, N.G., von Zastrow, M., 2014. Spatial encoding of cyclic AMP signaling specificity by GPCR endocytosis. Nature chemical biology 10(12), 1061-1065.

Turner, J.H., Gelasco, A.K., Raymond, J.R., 2004. Calmodulin interacts with the third intracellular loop of the serotonin 5-hydroxytryptamine1A receptor at two distinct sites: putative role in receptor phosphorylation by protein kinase C. The Journal of biological chemistry 279(17), 17027-17037.

Vilardaga, J.P., Bunemann, M., Krasel, C., Castro, M., Lohse, M.J., 2003. Measurement of the millisecond activation switch of G protein-coupled receptors in living cells. Nature biotechnology 21(7), 807-812.

Vilardaga, J.P., Romero, G., Feinstein, T.N., Wehbi, V.L., 2013. Kinetics and dynamics in the G protein-coupled receptor signaling cascade. Methods in enzymology 522, 337-363.

Ward, R.J., Milligan, G., 2014. Structural and biophysical characterisation of G protein-coupled receptor ligand binding using resonance energy transfer and fluorescent labelling techniques. Biochimica et biophysica acta 1838(1 Pt A), 3-14.

Williams, C., Hill, S.J., 2009. GPCR signaling: understanding the pathway to successful drug discovery. Methods in molecular biology 552, 39-50.

Xu, T.R., Ward, R.J., Pediani, J.D., Milligan, G., 2012. Intramolecular fluorescence resonance

energy transfer (FRET) sensors of the orexin OX1 and OX2 receptors identify slow kinetics of agonist activation. The Journal of biological chemistry 287(18), 14937-14949.

Yu, B., Wang, X., Wei, S., Fu, T., Dzakah, E.E., Waqas, A., Walthall, W.W., Shan, G., 2017. Convergent Transcriptional Programs Regulate cAMP Levels in C. elegans GABAergic Motor Neurons. Developmental cell 43(2), 212-226 e217.

Zadran, S., Standley, S., Wong, K., Otiniano, E., Amighi, A., Baudry, M., 2012. Fluorescence resonance energy transfer (FRET)-based biosensors: visualizing cellular dynamics and bioenergetics. Applied microbiology and biotechnology 96(4), 895-902.

Zheng, H., Loh, H.H., Law, P.Y., 2008. Beta-arrestin-dependent mu-opioid receptor-activated extracellular signal-regulated kinases (ERKs) Translocate to Nucleus in Contrast to G protein-dependent ERK activation. Molecular pharmacology 73(1), 178-190.

Zoghbi, M.E., Mok, L., Swartz, D.J., Singh, A., Fendley, G.A., Urbatsch, I.L., Altenberg, G.A., 2017. Substrate-induced conformational changes in the nucleotide-binding domains of lipid bilayer-associated P-glycoprotein during ATP hydrolysis. The Journal of biological chemistry 292(50), 20412-20424.

Figure legends

Figure 1 WIN-55212 induced changes in FRET signal from YFP/CFP-labeled CB1 receptor sensor. (A and B). Schematic illustrations of the FRET-based CB1 sensor. (C). eCFP and eYFP fluorescence showing effective delivery of the sensor to Flp-In ™ T-REx ™ 293 cells and successful induction by doxycycline. (D). mGluR5-VSV-G-CB1-M-YFP-CFP was induced in Flp-In™ T-REx™ 293 cells for FRET imaging studies. Various concentrations (10^{-5}M, 10^{-6} M, 10^{-7} M, 10^{-8} M, 10^{-9} M and 0 M) of WIN-55212-2 were added and FRET signal was monitored for 15 s. WIN-55212-2 was washed out for 15 s after application. (E). Cells expressing the CB1 sensor were pre-treated with 10^{-6} M rimonabant for 20 min and investigated as described in (D). Data represent mean ± SE, n=5.

Figure 2 Effects of different agonists on the CB1 FRET sensor. Cells expressing the CB1 sensor were used in FRET imaging studies. 10^{-6}M arachidonylethanolamide (A) and CP-55940 (B) were added at the indicated time points and the FRET signal was monitored for 45 s. The agonists were washed out for 15 s after application (bar). (C-D). Cells expressing the CB1 sensor were pre-treated with 10^{-6} M Org27569 (C) or taranabant (D) for 20 min and 10^{-6} M of WIN-55212-2 was added at the indicated time point and the FRET signal was monitored for 15 s. Data represent mean ± SE, n=5.

Figure 3 CB1 receptor sensor induces Ca^{2+} mobilization upon agonist binding. (A). Cells were treated with WIN-55212 for 60 s. Arrows indicate time of additions. (B). Cells were treated with 10^{-6}M arachidonylethanolamide (ARA) for 60 s. (C). Cells were treated with 10^{-6}M CP-55940 (CPA) for 60 s. (D). Cells were pre-treated with 10^{-6}M Org27569 (ORG) for 20 min, then treated with WIN-55212 for 60 s. Arrows indicate time of WIN-55212 addition. (E). Cells were pre-treated with 10^{-6}M taranabant (Tar) for 20 min, then treated with WIN-55212 for 60 s. Arrows indicate the time of WIN-55212 addition. n = 3. RFU = relative fluorescence units.

Figure 4 Internalization of the CB1-YFP/CFP biosensor in response to WIN-55212-2. (A). CFP fluorescence was detected in Flp-In™ T-REx™ 293 cells expressing mGluR5-VSV-

G-CB1-M-YFP-CFP at various times points following WIN-55212-2 (10^{-6} M) addition. (B and C). Cell surface biotinylation studies were performed on Flp-In^{TM}T-REx^{TM} 293 cells expressing mGluR5-VSV-G-CB1-M-YFP-CFP. The induced cells were treated with 1×10^{-6} M WIN-55212-2 for varying times (B) or with different concentrations of WIN-55212-2 for 40 min (C). Examples shown are representative of n=3 independent experiments.

Figure 5 Ability of the CB1-eYFP/eCFP biosensor to induce downstream ERK 1/2 phosphorylation after treatment with agonist. Cells expressing the CB1-YFP-CFP intramolecular sensor were treated with various concentrations of WIN-55212-2 (A and B) or ARA (C and D) for 5 min. The effects of WIN-55212-2 (A) or ARA (C) on VSV-G tagged expression were assessed by western blotting. CB1-YFP-CFP intramolecular sensor cells were serum-starved for 12 h then stimulated with various concentrations of WIN-55212-2 (B) or ARA (D) for 5 min. The expression of phosphorylated ERK (p-ERK) and total ERK was analyzed by western blotting.

Figure 6 CB1-YFP/CFP biosensor blockade restricts downstream ERK phosphorylation. Serum-starved CB1-YFP-CFP sensor expressing cells were pre-treated with 10^{-6} M rimonabant for 20 min. Cells were then stimulated with 10^{-6} M WIN-55212-2 (A), ARA (B), or CPA (C) for the indicated time periods. Phosphorylated ERK (p-ERK) and total ERK were analyzed by western blotting. (D) C257A and C264A mutations were introduced into the CB1 receptor intramolecular FRET sensor. Cells able to express the variant in response to doxycycline were generated. Phosphorylation of ERK1/2 in the presence of C257A and C264A mutations was analyzed by western blotting.

Fig.1

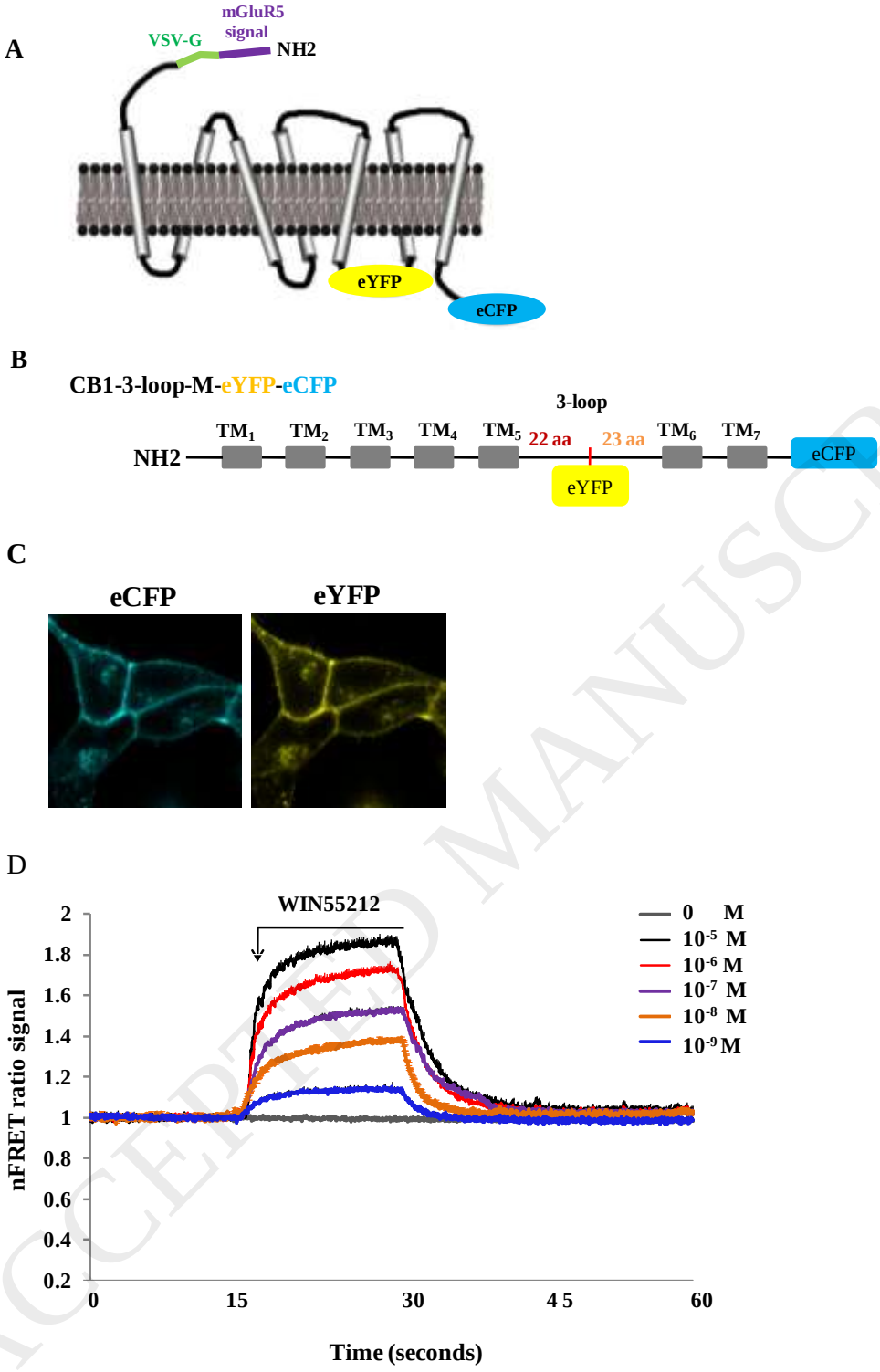

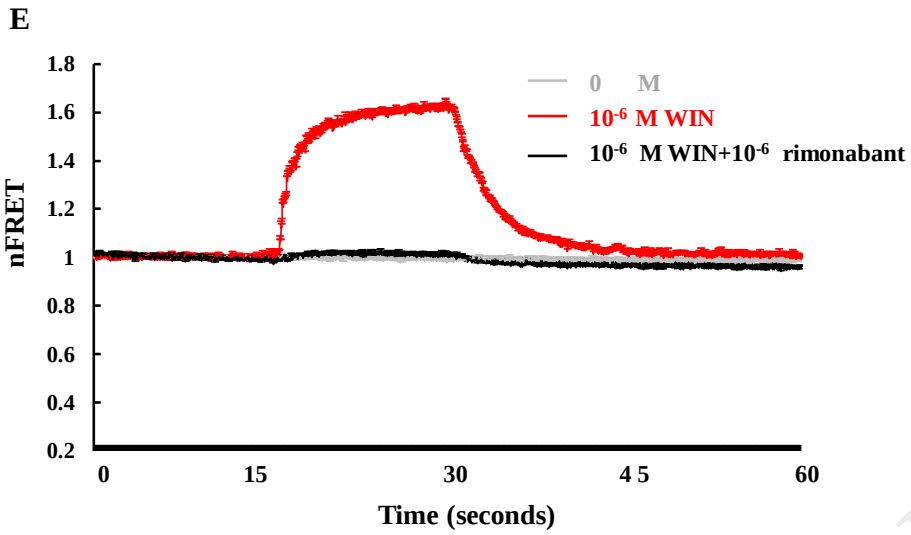

Fig.2

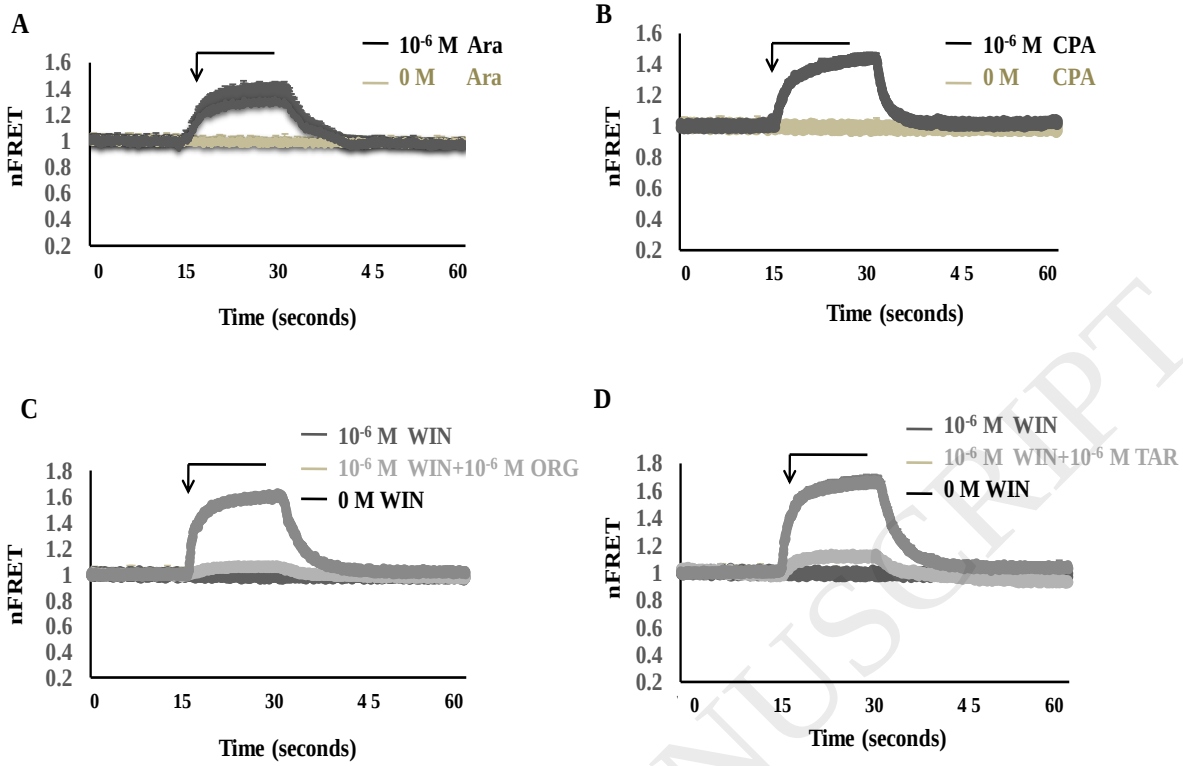

Fig.3

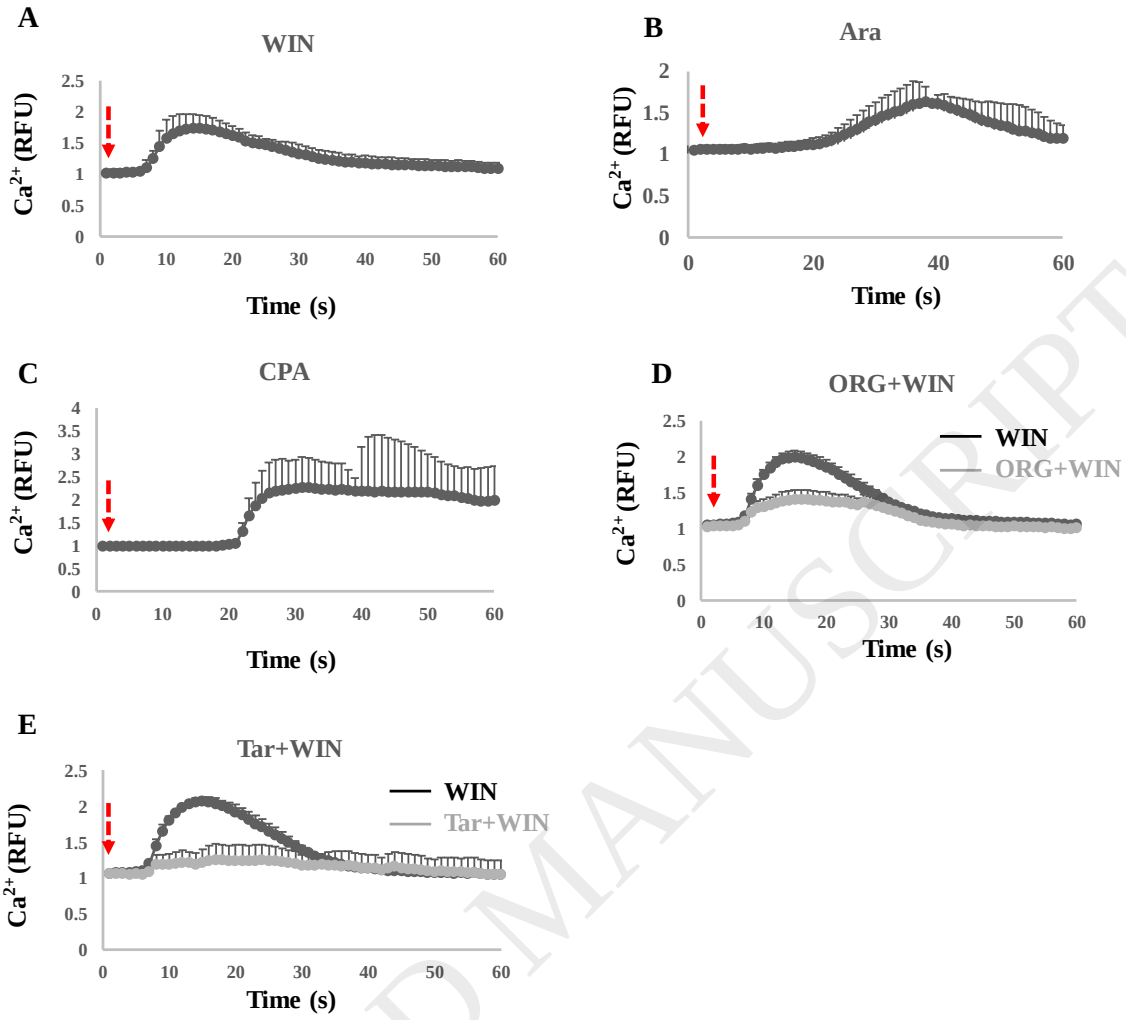

Fig.4

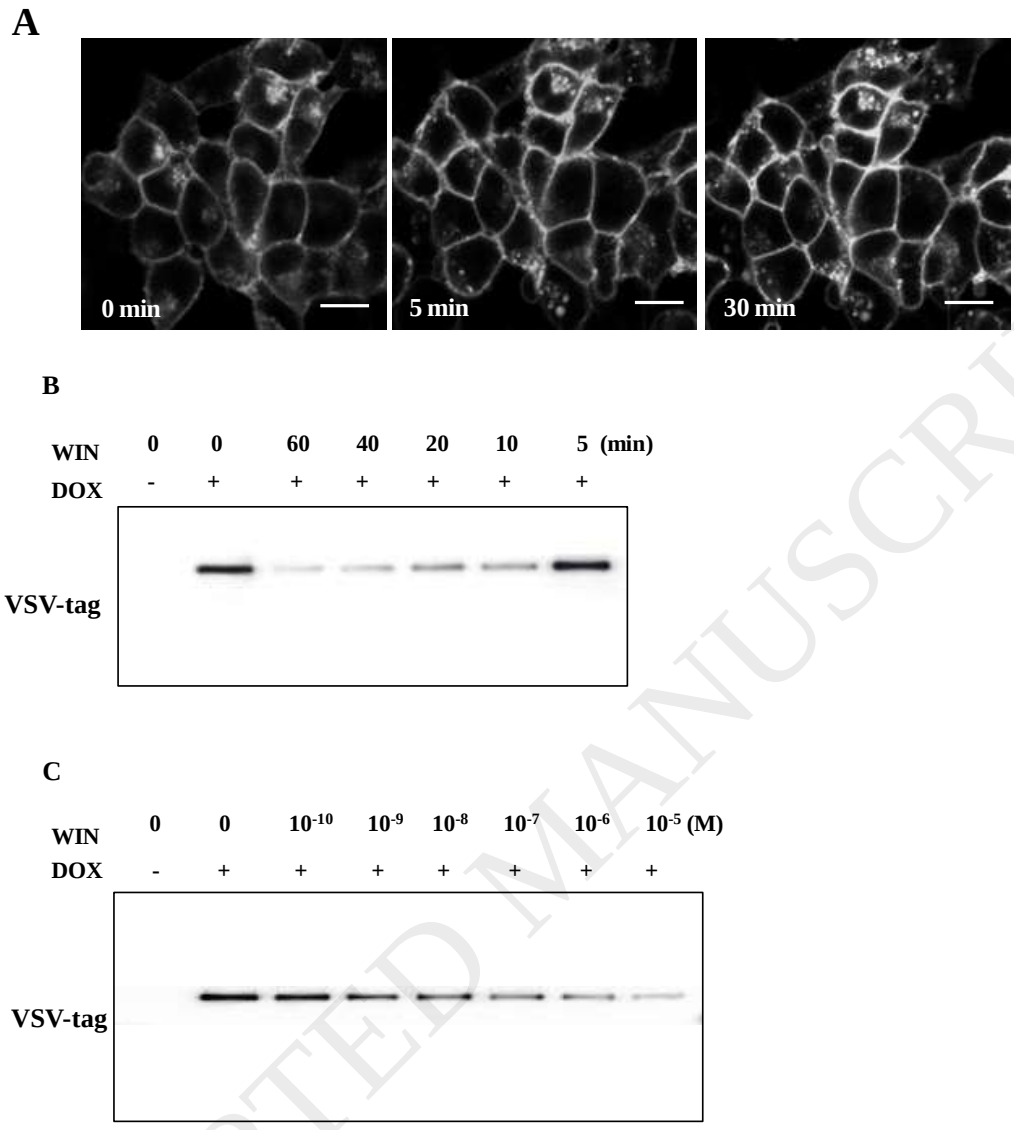

Fig.5

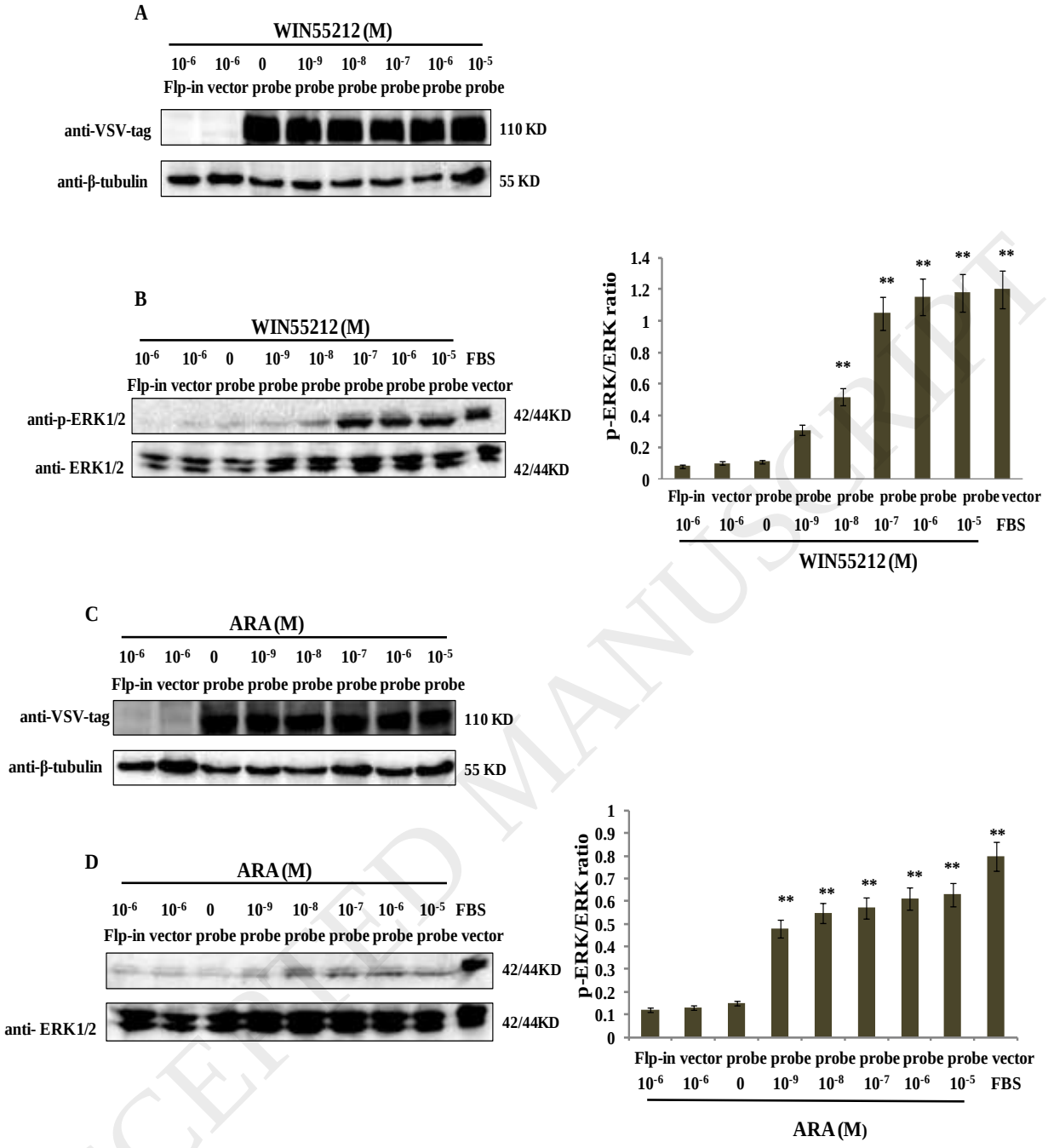

Fig.6

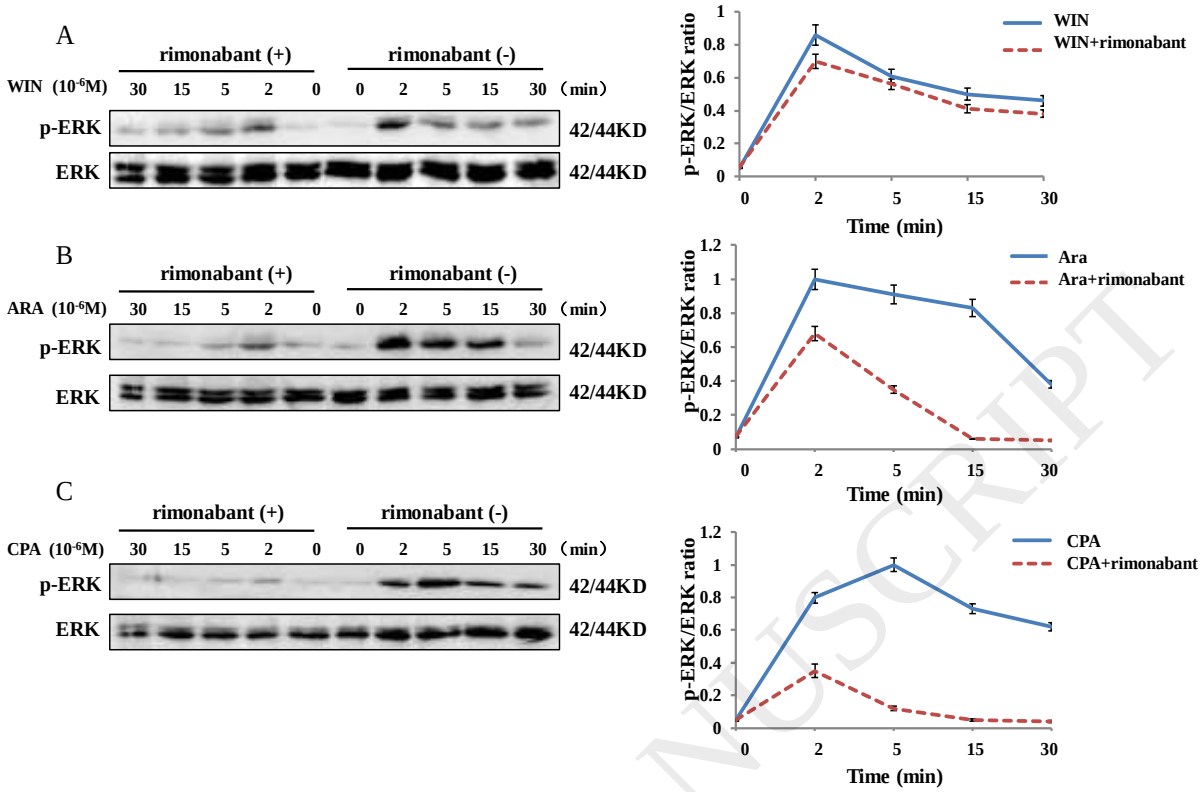

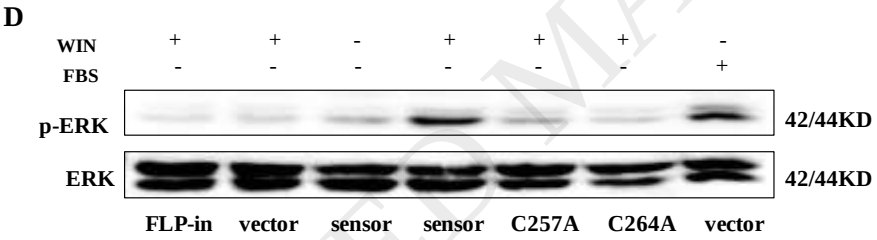

Table. 1 Binding characteristics of WIN-55212-2 to the CB1 FRET sensor expressed in Flp-in 293 cells.

WIN-55212-2 (M)	Kon ($10^5M^{-1}S^{-1}$)	Koff ($10^{-3}S^{-1}$)	Kd (nM)
10^{-5}	0.5773±0.013	0.3099±0.007	5.3675±0.025
10^{-6}	0.5475±0.044	0.3869±0.039	7.0673±0.012
10^{-7}	0.4027±0.023	0.3145±0.012	7.8090±0.016
10^{-8}	0.3629±0.021	0.3145±0.011	8.666±0.025
10^{-9}	0.7073±0.002	0.5656±0.025	7.9965±0.026

Binding parameters were calculated using Prism 5.0 software. Data are expressed as the mean ± SE of three or more independent experiments.

Table.2 Binding characteristics of agonists to the CB1 FRET sensor expressed in Flip-in 293 cells.

Agonist (10^{-6} M)	Kon ($10^5M^{-1}S^{-1}$)	Koff ($10^{-3}S^{-1}$)	Kd (nM)
Ara	3.085±0.008	0.219±0.005	7.108±0.062
CPA	3.539±0.002	0.441±0.005	12.461±0.025

Binding parameters were calculated using Prism 5.0 software. Data are expressed as the mean ± SE of three or more independent experiments.

Ara, Arachidonylethanolamide; CPA, CP-55940; ORG, Org27569; TAR, Taranabant;